

Diffusion Models for Video Prediction and Infilling

Tobias Höppe¹, Arash Mehrjou^{*,2,3}, Stefan Bauer^{*,1}, Didrik Nielsen^{*,4}, Andrea Dittadi^{*,2,5}

¹KTH Stockholm, ²Max Planck Institute for Intelligent Systems, Tübingen, Germany,

³ETH Zürich, ⁴Norwegian Computing Center, ⁵Technical University of Denmark

Abstract

To predict and anticipate future outcomes or reason about missing information in a sequence is a key ability for agents to be able to make intelligent decisions. This requires strong temporally coherent generative capabilities. Diffusion models have shown huge success in several generative tasks lately, but have not been extensively explored in the video domain. We present Random-Mask Video Diffusion (RaMViD), which extends image diffusion models to videos using 3D convolutions, and introduces a new conditioning technique during training. By varying the mask we condition on, the model is able to perform video prediction, infilling and upsampling. Since we do not use concatenation to condition on a mask, as done in most conditionally trained diffusion models, we are able to decrease the memory footprint. We evaluated the model on two benchmark datasets for video prediction and one for video generation on which we achieved competitive results. On Kinetics-600 we achieved state-of-the-art for video prediction.

1. Introduction

Videos contain rich information about the world, and a vast amount of diverse video data is available. Training models that understand this data can be crucial for developing agents that interact with the surrounding world effectively. In particular, video prediction plays an increasingly important role: Autonomous driving (Hu et al., 2020), anticipating events (Zeng et al., 2017), planning (Finn and Levine, 2017) and reinforcement learning (Hafner et al., 2019) are applications which can benefit from increasing performance of prediction models. On the other hand, video infilling—i.e., observing a part of a video and generating missing frames—can be used in planning, estimating trajectories, and video processing. In addition, video models can be valuable for downstream tasks such as action recognition (Kong and Fu, 2018) and pose estimation (Sahin et al., 2020). However, there has not been extensive research on video infilling and most research is focusing on generation or prediction.

Most recent approaches to video prediction have used variational autoencoders (Babaeizadeh et al., 2021; Saxena, Ba, and Hafner, 2021) or GANs (Clark, Donahue, and Simonyan, 2019; Luc et al., 2020). Diffusion models (Abstreiter et al., 2021; Dockhorn, Vahdat, and Kreis, 2021; Ho, Jain, and Abbeel, 2020; Mittal et al., 2022; Nichol and Dhariwal, 2021; Sohl-Dickstein et al., 2015; Song et al., 2021) have recently seen tremendous progress on static visual data, even outperforming GANs in image synthesis (Dhariwal and Nichol, 2021), but have not yet been extensively studied for videos. Considering their impressive performance on images, it is reasonable to believe that diffusion models may also be useful for tasks in the video domain.

In this paper, we extend diffusion models to the video domain via several technical contributions. We use 3D convolutions and a new conditioning procedure incorporating randomness. Our model is not only able to predict future frames of a video but also fill in missing frames at arbitrary positions.

*Equal advising.

Therefore, our Random-Mask Video Diffusion (RaMViD) can be used for several video completion tasks.¹ We summarize our technical contributions as follows:

- A novel diffusion-based architecture for video prediction and infilling.
- Competitive performance with recent approaches across multiple datasets.
- Introduce a schedule for the random masking.

The remainder of this paper is organized as follows: In Section 2, we provide the necessary background on diffusion models and video prediction and outline relevant related work. Section 3 describes Random-Mask Video Diffusion (RaMViD). In Section 4, we present and discuss extensive experiments on several benchmark datasets. We finally conclude with a discussion in Section 5.

2. Background and related work

Diffusion models. Diffusion-based models generally refer to the class of machine learning algorithms that consist of gradually transforming a complex distribution into unstructured noise and learning to reverse this process to recover the data generating distribution. They have attracted a great deal of attention after being successfully applied to a diverse range of tasks such as image generation (Niu et al., 2020; Song et al., 2021), audio (Chen et al., 2021), graph and shape generation (Cai et al., 2020). The essence of these models is two stochastic (diffusion) processes implemented by Stochastic Differential Equations (SDEs), a forward and a backward one. We explain the formulation in the abstract domain here and specialize it later according to the application of this work.

Let $\mathbf{x}_0 \in \mathbb{R}^d$ be a sample from the empirical data distribution, i.e., $\mathbf{x}_0 \sim p_{\text{data}}(\mathbf{x}_0)$ and d be the data dimension. The forward diffusion process takes \mathbf{x}_0 as the starting point and creates the random trajectory $\mathbf{x}_{[0,T]}$ from $t = 0$ to the final time $t = T$. The forward process is designed such that $p(\mathbf{x}_T | \mathbf{x}_0)$ has a simple unstructured distribution. One example of such SDEs is

$$d\mathbf{x}_t = f(\mathbf{x}_t, t)dt + g(t)dw := \sqrt{\frac{d[\sigma^2(t)]}{dt}}dw, \quad (1)$$

where w is the Brownian motion. A desirable property of this process is the fact that the conditional distribution $p(\mathbf{x}_t | \mathbf{x}_0)$ takes a simple analytical form:

$$p(\mathbf{x}_t | \mathbf{x}_0) = \mathcal{N}(\mathbf{x}_t; \mathbf{x}_0, (\sigma^2(t) - \sigma^2(0))\mathbf{I}). \quad (2)$$

Upon learning the gradient of $p(\mathbf{x}_t)$ for each t , one can reverse the above process and obtain the complex data distribution from pure noise as

$$d\mathbf{x}_t = [f(\mathbf{x}_t, t) - g^2(t)\nabla_{\mathbf{x}} \log p(\mathbf{x}_t)]dt + g(t)dw', \quad (3)$$

where w' is a Brownian motion independent of the one in the forward direction. Hence, generating samples from the data distribution boils down to learning $\nabla_{\mathbf{x}} \log p(\mathbf{x})$.

The original score matching objective (Hyvärinen and Dayan, 2005):

$$\mathbb{E}_{\mathbf{x}_t} [\|s_\theta(\mathbf{x}_t, t) - \nabla_{\mathbf{x}_t} \log p(\mathbf{x}_t)\|_2^2] \quad (4)$$

is the most intuitive way to learn the score function, but is unfortunately intractable. Denoising Score Matching (DSM) provides a tractable alternative objective function:

$$J_t^{DSM}(\theta) = \mathbb{E}_{\mathbf{x}_0} \mathbb{E}_{\mathbf{x}_t | \mathbf{x}_0} [\|s_\theta(\mathbf{x}_t, t) - \nabla_{\mathbf{x}_t} \log p(\mathbf{x}_t | \mathbf{x}_0)\|_2^2] \quad (5)$$

¹High resolution videos are provided at <https://sites.google.com/view/video-diffusion-prediction>.

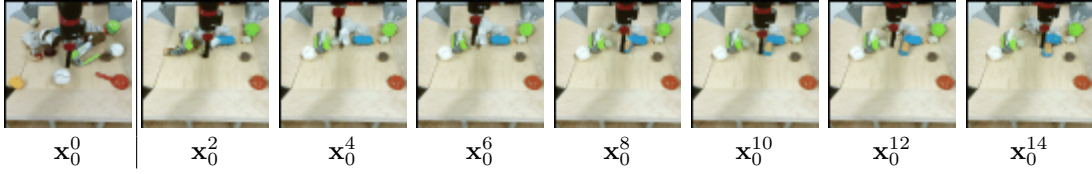


Figure 1: An unconditionally trained model is used to predict 15 frames given one frame. Even with re-sampling we can see, that objects in the background are not harmonized between the predicted and conditioning frames.

whose equivalence with the original score matching objective was shown by Vincent (2011) and used to train energy models in Saremi et al. (2018). Similar to many recent works, we use the DSM formulation of score matching in this work to learn the score function.

Video prediction and infilling. Research in video prediction has gotten more attention in the previous years, as the ability to predict videos can be used for several downstream tasks (Oprea et al., 2020). Video prediction can be modeled in a deterministic or stochastic form. Deterministic modeling (Sun et al., 2019; Terwilliger, Brazil, and Liu, 2019; Vondrick and Torralba, 2017; Walker, Gupta, and Hebert, 2015) tries to predict the most likely future, but this often leads to averaging the future states (Li et al., 2019). Due to the stochastic nature of the future, generative models have lately shown to be more successful in capturing the underlying dynamics. For this approach, variational models are often used by modeling the stochastic content in a latent variable (Babaeizadeh et al., 2018; Denton and Fergus, 2018; Saxena, Ba, and Hafner, 2021; Wu et al., 2021a). However, this often leads to blurry prediction by underfitting and Babaeizadeh et al. (2021) have overcome this problem by architectural novelties. The blurry prediction is a less serious problem in GANs and promising results have been achieved especially on large datasets (Clark, Donahue, and Simonyan, 2019; Luc et al., 2020). On the other hand, the body of research on video infilling is significantly more scarce, with most works in this area focusing on frame interpolation (Jiang et al., 2018). However, Xu et al. (2018) have shown interesting results in infilling, by modeling the video as a stochastic generation process.

Concurrent work. Yang, Srivastava, and Mandt (2022) is the only work so far that has used diffusion models for autoregressive video prediction, by modeling residuals for a predicted frame. However, since their evaluation procedure and datasets are different, a comparison with their work is not possible. A few concurrent works have recently considered diffusion models for video generation. Ho et al. (2022) focus on unconditional video generation, Harvey et al. (2022) use diffusion models to predict long videos, and Voleti, Jolicoeur-Martineau, and Pal (2022), the most similar to our work, also consider video prediction and infilling.

3. Random-Mask Video Diffusion

Our method, Random-Mask Video Diffusion (RaMViD), consists of two main features. First, the way we introduce conditional information to the network is different from what has been used so far. Second, by randomizing the mask, we can directly use the same approach for video prediction and video completion (infilling). In the following, we detail each of these aspects of the proposed method.

3.1 Conditional training

Let $\mathbf{x}_0 \in \mathbb{R}^{L,W,H,C}$ be a video with length L . We partition the video \mathbf{x}_0 into two parts, the unknown frames $\mathbf{x}_0^{\mathcal{U}} \in \mathbb{R}^{L-k,W,H,C}$ and the conditioning frames $\mathbf{x}_0^{\mathcal{C}} \in \mathbb{R}^{k,W,H,C}$, where \mathcal{U} and \mathcal{C} are sets of indices such that $\mathcal{U} \cap \mathcal{C} = \emptyset$ and $\mathcal{U} \cup \mathcal{C} = \{0, 1, \dots, L-1\}$. We write $\mathbf{x}_0 = \mathbf{x}_0^{\mathcal{U}} \oplus \mathbf{x}_0^{\mathcal{C}}$ with the following definition for the \oplus operator:

$$(\mathbf{a}^{\mathcal{U}} \oplus \mathbf{b}^{\mathcal{C}})^i := \begin{cases} \mathbf{a}^i & \text{if } i \in \mathcal{U} \\ \mathbf{b}^i & \text{if } i \in \mathcal{C} \end{cases} \quad (6)$$

where the superscript i indicates tensor indexing and in our case corresponds to selecting a frame from a video. Here, t indicates the diffusion step, with $t = 0$ corresponding to the data and $t = T$ to the prior Gaussian distribution.

If we use an unconditionally trained model, we find that the predicted unknown frames $\mathbf{x}_0^{\mathcal{U}}$ do not harmonize well with the conditioning frames $\mathbf{x}_0^{\mathcal{C}}$ (Fig. 1). One solution for this would be re-sampling, as proposed by Lugmayr et al. (2022). In re-sampling, we take one step in the learned reversed diffusion (denoising) process and then go back by taking a step in the diffusion process (i.e., adding noise again). This is done several times for each diffusion step, to make sure the model harmonizes between the predicted and conditioning frames. However, this becomes computationally too expensive for videos, especially when using very few conditioning frames, as the number of re-sampling steps need to be increased. To mitigate this issue, we propose to train the model conditionally with *randomized masking*.

Conditional diffusion models usually optimize

$$\mathbb{E}_{\mathbf{x}_0} \left\{ \mathbb{E}_{\mathbf{x}_t | \mathbf{x}_0} \left[\left\| s_{\theta}(\mathbf{x}_t, \mathbf{x}_0^{\mathcal{C}}, t) - \nabla_{\mathbf{x}_t} \log p(\mathbf{x}_t | \mathbf{x}_0) \right\|_2^2 \right] \right\} \quad (7)$$

where $\mathbf{x}_0^{\mathcal{C}}$ is typically given as a separate input through an additional layer (Chen et al., 2021) or it is expanded to the dimension of \mathbf{x}_t (e.g., via padding) and concatenated with the input (Batzolis et al., 2021; Saharia et al., 2021a; b). For videos, this would significantly increase the memory footprint. Therefore, we feed the entire sequence to the network s_{θ} but only add noise to the unmasked frames: $\mathbf{x}_t^{\mathcal{U}} \sim \mathcal{N}(\mathbf{x}_0^{\mathcal{U}}, (\sigma^2(t) - \sigma^2(0)) \mathbf{I})$. We then calculate the loss only on that part of the video. The input to the network is then a video where some frames are noisy and some are clean: $\mathbf{x}_t = \mathbf{x}_t^{\mathcal{U}} \oplus \mathbf{x}_0^{\mathcal{C}}$ (see Fig. 2). The loss is computed only with respect to $\mathbf{x}_t^{\mathcal{U}}$:

$$J_t^{\text{RaMViD}}(\theta) = \mathbb{E}_{\mathbf{x}_0} \left\{ \mathbb{E}_{\mathbf{x}_t^{\mathcal{U}} | \mathbf{x}_0} \left[\left\| s_{\theta}(\mathbf{x}_t, t)(\mathbf{x}_t^{\mathcal{U}}) - \nabla_{\mathbf{x}_t^{\mathcal{U}}} \log p(\mathbf{x}_t^{\mathcal{U}} | \mathbf{x}_0) \right\|_2^2 \right] \right\}. \quad (8)$$

Note that the score function $\nabla_{\mathbf{x}_t^{\mathcal{U}}} \log p(\mathbf{x}_t^{\mathcal{U}} | \mathbf{x}_0)$ has the same dimension as $\mathbf{x}_t^{\mathcal{U}}$, whereas in Eq. (7) it had the dimension of the entire video \mathbf{x}_t . The reversed diffusion process then becomes:

$$d\mathbf{x}_t^{\mathcal{U}} = [f(\mathbf{x}_t^{\mathcal{U}}, t) - g^2(t) \nabla_{\mathbf{x}_t^{\mathcal{U}}} \log p(\mathbf{x}_t^{\mathcal{U}} | \mathbf{x}_0^{\mathcal{C}})] dt + g(t) dw' \quad (9)$$

Similarly, Tashiro et al. (2021) calculate the loss only with respect to the unknown input, however, they also use concatenation and zero-padding to bring $\mathbf{x}_t^{\mathcal{C}}$ and \mathbf{x}_t to the same dimension. For a more detailed schematic see Appendix A.1. For our implementation we used the discrete diffusion process with $t \in \{0, 1, \dots, T-1, T\}$.

3.2 Randomization

As mentioned, the model is able to perform several tasks. We achieve this by choosing \mathcal{C} at random. At each training step, we first choose the number of conditioning frames $|\mathcal{C}| = k \in \{1, \dots, K\}$, where

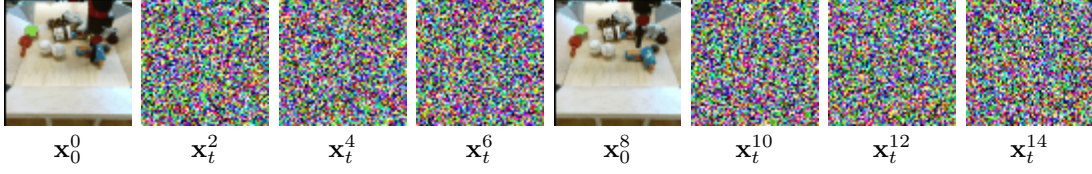


Figure 2: Example input of the network with $\mathcal{C} = \{0, 8\}$.

K is a chosen hyper-parameter. Then we choose k random indices from $\{0, \dots, L - 1\}$, which we do not diffuse. Since the video now consists of original and diffused frames in varying positions the model has to learn to distinguish between those in order to use the frames $\mathbf{x}_0^{\mathcal{C}}$ as information for the reversed diffusion process. Our approach allows us to use the exact same architecture as for unconditionally trained models, since we only have to make some changes to the diffusion process and the loss. The pseudocode for RaMViD can be found in Algorithm 1.

We can also perform *mixed training*: instead of always having at least one frame on which we can condition, we choose $k \in \{0, \dots, K\}$, i.e., we allow $\mathcal{C} = \emptyset$. Therefore, the model also has to learn the unconditional reversed diffusion without any additional information $\mathbf{x}_t^{\mathcal{C}}$. We conduct a study on this in Section 4.5.

Algorithm 1 RaMViD.

```

Initialize model  $\sim s_\theta$ 
 $T$  = Number of diffusion steps
 $K$  = Max number of frames to condition on
 $L$  = Length of the video
while not converged do
     $\mathbf{x}_0 \sim p_{\text{data}}(\mathbf{x}_0)$  ▷ sample data point
     $t \sim \text{Uniform}(\{0, \dots, T\})$ 
     $k \sim \text{Uniform}(\{1, \dots, K\})$ 
     $\mathcal{C} \sim \text{Uniform}(\{S \subseteq \{0, \dots, L - 1\} : |S| = k\})$  ▷ choose  $k$  conditioning frames
     $\mathcal{U} = \{0, \dots, L - 1\} \setminus \mathcal{C}$ 
     $\mathbf{x}_t^{\mathcal{U}} \sim \mathcal{N}(\mathbf{x}_t^{\mathcal{U}}; \mathbf{x}_0^{\mathcal{U}}, (\sigma^2(t) - \sigma^2(0)) \mathbf{I})$ 
     $\mathbf{x}_t = \mathbf{x}_t^{\mathcal{U}} \oplus \mathbf{x}_0^{\mathcal{C}}$ 
    Take gradient step on  $\nabla_\theta \mathbb{E}_{\mathbf{x}_0} \left\{ \mathbb{E}_{\mathbf{x}_t^{\mathcal{U}} | \mathbf{x}_0} \left[ \left\| s_\theta(\mathbf{x}_t, t)(\mathbf{x}_t^{\mathcal{U}}) - \nabla_{\mathbf{x}_t^{\mathcal{U}}} \log p(\mathbf{x}_t^{\mathcal{U}} | \mathbf{x}_0) \right\|_2^2 \right] \right\}$ 
end while

```

4. Experiments

4.1 Experimental setup

Implementation details. Our implementation relies on the official code of Nichol and Dhariwal (2021).² Even though most previous work uses the cosine noise schedule, we found that the linear noise schedule works better when training the model conditionally. Therefore, we use a linear diffusion schedule for our experiments unless otherwise stated. For the architecture, we also use the same as proposed by Nichol and Dhariwal (2021): a U-Net with self-attention at the resolutions 16 and 8. We do not encode the time dimension. We use two ResNet blocks per resolution for the BAIR dataset,

²<https://github.com/openai/improved-diffusion>

and three blocks for Kinetics-600 and UCF-101. We set the learning rate for all our experiments to $2e-5$, use a batch size of 32 for BAIR and 64 for Kinetics-600 and UCF-101 and use $T = 1000$. We found, especially on the more diverse datasets like Kinetics-600 and UCF-101, that larger batch sizes produce better results. Therefore, to increase the batch size, we use gradient accumulation by computing the gradients for four micro-batches of size 8 (BAIR) or 16 (Kinetics-600, UCF-101) before doing back-propagation.

Datasets and evaluations. To compare our model to prior work, we train it on the BAIR robot pushing dataset (Ebert et al., 2017). The dataset consists of short videos, with 64×64 resolution, of a robot arm manipulating different objects. We use the same preprocessing pipeline as Yan et al. (2021), available at the corresponding public repository.³ For evaluation, we use the same setting as Rakhimov et al. (2020), which is to predict the next 15 frames given one observed frame. We train on a sequence length of 20 and choose $K = 4$.

Additionally, we evaluate our model on the Kinetics-600 dataset (Carreira et al., 2018), which consists of roughly 500,000 10-second YouTube clips, also at 64×64 resolution, from 600 classes. The size and the diversity of this dataset make it a perfect task to investigate if the model captures the underlying real-world dynamics. For downloading and preprocessing we use the dataset’s public repository.⁴ On Kinetics-600, we compare our model to concurrent work by predicting 11 frames when conditioned on 5 frames (Luc et al., 2020). We additionally perform several ablation studies on video completion. We train on 16 frames and choose again $K = 4$.

To test if the model is also able to generate videos unconditionally, we test *mixed training* (i.e., allowing $\mathcal{C} = \emptyset$) on UCF-101 (Soomro, Zamir, and Shah, 2012), a common dataset for unconditional video generation. It consists of 13,320 videos from 101 human action classes. We also rescale this dataset to 64×64 and train with $K = 2$. We only train on 13,118 videos, to have a test set on which we can evaluate conditional generation.

To quantitatively evaluate prediction, we use the Fréchet Video Distance (FVD) (Untertiner et al., 2018),⁵ which captures semantic similarity and temporal coherence between videos by comparing statistics in the latent space of a Inflated 3D ConvNet (I3D) trained on Kinetics-400. To evaluate unconditional generation, we use the Inception Score (IS) Salimans et al. (2016) to measure the quality and diversity of the generated videos. As we have to adapt the score to videos, we use the public repository from Saito et al. (2020).⁶

4.2 Prediction

We test the video prediction capabilities of RaMViD on the BAIR and Kinetics-600 datasets. On BAIR, the evaluation procedure consists in predicting 15 frames given one conditioning frame. Since the movements of the robot arm are mostly random and we have only one frame to condition on, this task is well suited to evaluate the generative performance of prediction models. We train our method in two different masking settings: *RaMViD*, described in Algorithm 1, where at each training step the mask is chosen at random with $K = 4$; and *RaMViD (fixed)* with task-specific masking, where we fix \mathcal{C} to the first frame (i.e., $\mathcal{C} = \{0\}$ for all training steps). For both models, we train on sequence with length $L = 20$ and use the network architecture described in Section 4.1. In Table 1, we report the performance of both our models compared to recent methods. While RaMViD achieves good performance and ranks second among recent work, RaMViD (fixed) performs significantly worse.

³<https://github.com/wilson1yan/VideoGPT>

⁴<https://github.com/cvdfoundation/kinetics-dataset>

⁵https://github.com/google-research/google-research/tree/master/frechet_video_distance

⁶<https://github.com/pfnet-research/tgan2>

Table 1: Prediction performance on BAIR. The values are taken from Babaeizadeh et al. (2021) after inquiring about the evaluation procedure.

Method	FVD (\downarrow)
Latent Video Transformer (Rakhimov et al., 2020)	125.8
SAVP (Lee et al., 2018))	116.4
DVD-GAN-FP (Clark, Donahue, and Simonyan, 2019)	109.8
TrIVD-GAN-FP (Luc et al., 2020)	103.3
VideoGPT (Yan et al., 2021)	103.3
Video Transformer (Weissenborn, Täckström, and Uszkoreit, 2020)	94.0
FitVid (Babaeizadeh et al., 2021)	93.6
NÜWA (Wu et al., 2021b)	86.9
RaMViD	89.23
RaMViD (fixed)	103.62

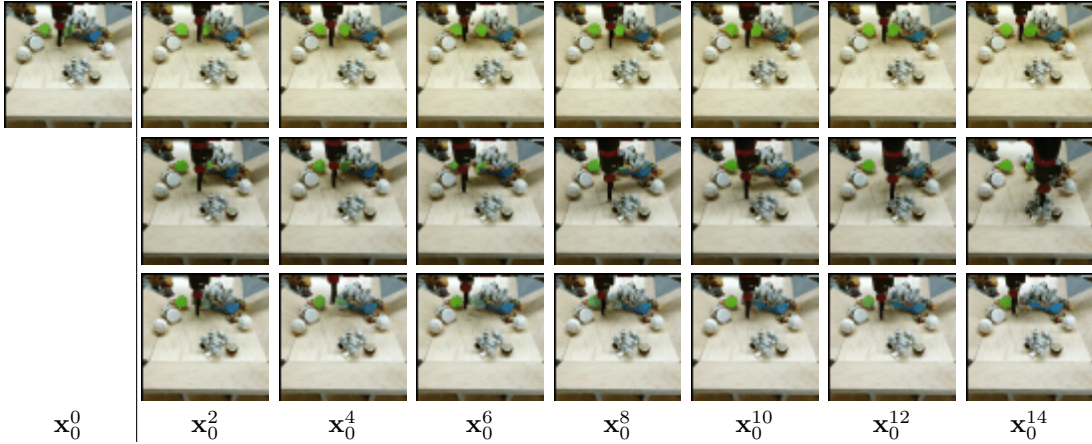


Figure 3: Three different predictions on BAIR given the same initial frame.

Another obvious shortcoming for RaMViD (fixed) is, that it is not able to solve several tasks, such as video infilling, given an arbitrary set of observed frames.

Qualitatively, we find that RaMViD can generate realistic and diverse predictions given the same conditioned frame (Fig. 3). However, we also observe two main shortcomings. First, sometimes the model changes the lighting of the video between the predicted and conditioning frames. Second, we sometimes observe unrealistic deformations of an object when it is moved by the robot arm.

On Kinetics-600, the evaluation task consists in predicting 11 frames given 5 conditioning frames. Unlike the BAIR dataset, which consists of random movements of the robot arm, Kinetics-600 videos display actions performed by humans. The model has to be able to complete the observed movements from the first five frames, which leaves less uncertainty in the predictions. For this experiment, we train with $L = 16$ and $K = 4$. As mentioned in Section 4.1, due to the high complexity of the dataset, we use three ResNet blocks per resolution, which increases the model size to approximately 665M parameters. RaMViD can achieve state-of-the-art results in prediction on Kinetics-600 (see Table 2). In Fig. 4, we can see that the model produces temporally coherent outputs and is able to model details, especially in the background, such as clouds and patterns in water. Nevertheless, we found the model sometimes struggles with fast movements: objects moving quickly often get deformed (see Appendix B.2).

Table 2: Prediction performance on Kinetics-600. Values are taken from Moing, Ponce, and Schmid (2021) after inquiring about the evaluation procedure.

Method	FVD (\downarrow)
Video Transformer (Weissenborn, Täckström, and Uszkoreit, 2020)	170 ± 5
DVD-GAN-FP (Clark, Donahue, and Simonyan, 2019)	69 ± 1
CCVS (Moing, Ponce, and Schmid, 2021)	55 ± 1
TrIVD-GAN-FP (Luc et al., 2020)	26 ± 1
RaMViD	22.51

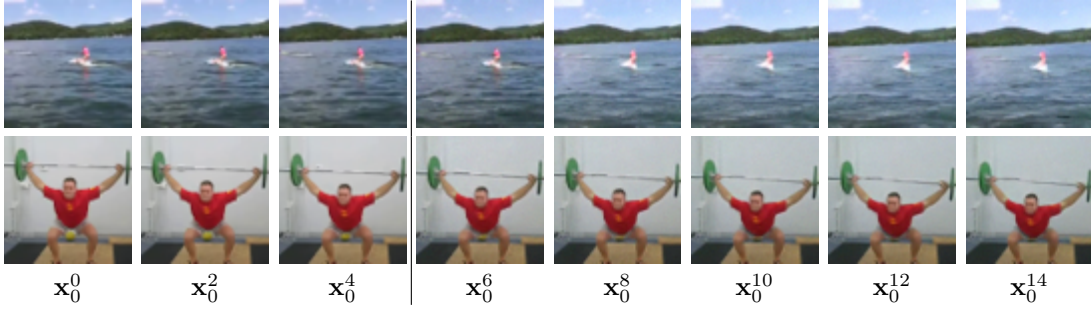


Figure 4: Prediction of 11 frames given the first 5 frames on Kinetics-600.

4.3 Infilling

Thanks to randomized masking, a single RaMViD model can solve several video completion tasks. Therefore, in this section, we use the model trained on Kinetics-600 for video prediction in Section 4.2, and evaluate it on two additional video completion tasks. The first setting is to fill in a video given the two first and last frames (i.e., $\mathcal{C} = \{0, 1, 14, 15\}$): the challenge here is to harmonize the observed movement at the beginning with the movement observed at the end. In the other setting, the conditioning frames are distributed evenly over the sequence (i.e., $\mathcal{C} = \{0, 5, 10, 15\}$), hence the model has to infer the movement from the static frames and harmonize them into one realistic video. This setting can be easily applied to upsampling by training a model on high-FPS videos and then sampling a sequence conditioned on a low-FPS video.

Note that we only condition on four frames and we calculate the FVD on the entire video, i.e., we also include the conditioning frames. Therefore, in Table 3, the model has to generate one more frame compared to the prediction task. However, the model excels in both evaluation settings in terms of FVD, but we find that it is much easier for the model to fill in the short missing sequences for $\mathcal{C} = \{0, 5, 10, 15\}$ than filling in one long sequence when $\mathcal{C} = \{0, 1, 14, 15\}$ (see Table 3). In addition, qualitatively we can see that the model can successfully harmonize the predicted and generated frames in both settings (see Fig. 5).

Table 3: Infilling performance of RaMViD on Kinetics-600, when conditioning on different frames.

Conditioning frames \mathcal{C}	FVD (\downarrow)
$\{0, 1, 14, 15\}$	22.03
$\{0, 5, 10, 15\}$	12.50



Figure 5: Filling a video when the first two and the last two frames are given.

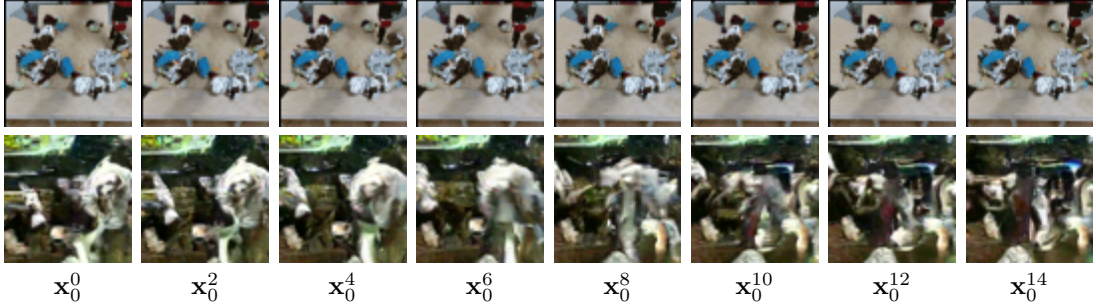


Figure 6: First row: Unconditional generation on the BAIR dataset sampled from RaMViD. Due to the low complexity of the dataset, we can generate reasonable unconditional videos. Second row: Unconditional generation on the Kinetics-600 dataset sampled from RaMViD. On this dataset unconditional generation does not work and the generated videos are mostly random color mixtures.

4.4 Unconditional generation

While RaMViD is not trained for unconditional generation, unconditional sampling with the model trained on BAIR (Section 4.2) yields reasonable videos. The robot arm and its movements are generated clearly, although the objects do not align with those seen in the training set (see Fig. 6, first row). The reverse diffusion process learned by the model appears to work relatively well even without conditioning frames. However, when sampling unconditionally from RaMViD trained on Kinetics-600, the model does not produce coherent videos. Most of the generated videos consist of random color mixtures—only a few videos contain recognizable objects such as humans or water, and even then, their quality is low (see Fig. 6, second row). We conjecture this may be due to the relatively low diversity in BAIR. These results motivated us to investigate whether it is possible to train RaMViD also for unconditional generation, while maintaining the good conditional generation capabilities observed so far. We will present and discuss our findings in the next section.

4.5 Mixed training

In the previous sections, we have observed that RaMViD succeeds at several video completion tasks, but in general it struggles with unconditional generation, especially on complex datasets. To enable the model to generate unconditional videos, we train in mixed mode, by choosing $k \in \{0, \dots, K\}$ instead of $k \in \{1, \dots, K\}$, i.e., allowing $\mathcal{C} = \emptyset$ during training. We call this setting *RaMViD (mixed)*.

When training RaMViD (mixed) on UCF-101, we use three ResNet blocks per resolution and videos of length $L = 16$. To strengthen the generative performance, we also decrease K and choose $K = 2$,

Table 4: Generative performance of hybrid RaMViD on UCF-101. Note that the methods VideoGPT and DVD-GAN in Table 4 are trained with 128×128 resolution, which gives them a slight advantage, as the IS score is computed with 112×112 resolution.

Method	IS (\uparrow)
VGAN (Vondrick, Pirsiavash, and Torralba, 2016)	8.31 ± 0.09
MoCoGAN (Tulyakov et al., 2018)	12.42 ± 0.03
TGAN-F (Kahembwe and Ramamoorthy, 2020)	13.62
progressive VGAN (Acharya et al., 2018)	14.56 ± 0.05
VideoGPT (Yan et al., 2021)	24.69 ± 0.3
TGANv2 (Saito et al., 2020)	26.60 ± 0.47
DVD-GAN (Clark, Donahue, and Simonyan, 2019)	32.97 ± 1.7
RaMViD (mixed)	18.9 ± 0.03

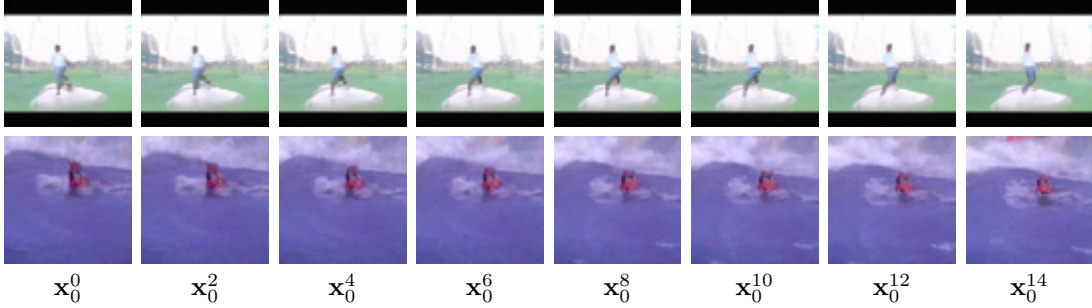


Figure 7: Unconditional generation on the UCF-101 dataset.

such that one in three times the model is actually trained as an unconditional model. Table 4 shows competitive performance on unconditional video generation, although we do not reach state-of-the-art. The trained models can successfully generate scenes with a static background and a human performing an action in the foreground, consistent with the training dataset. However, the actions are not always coherent and moving objects can deform over time (see Fig. 7). RaMViD (mixed) can also be used for video infilling (see Fig. 8). For quantitative results on prediction and infilling, we refer to Appendix B.3.

We also train RaMViD (mixed) on the Kinetics-600 dataset to evaluate how the mixed training affects the prediction task. We choose the same masking parameters as for RaMViD (mixed) on

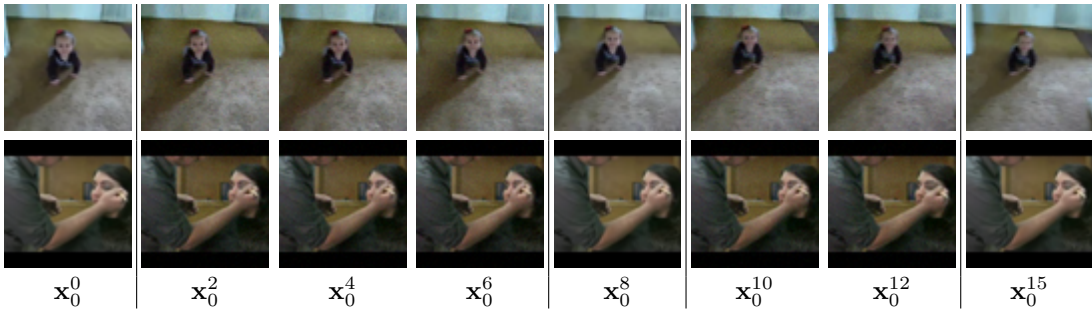


Figure 8: Infilling on the UCF-101 dataset. In this setting we chose $\mathcal{C} = \{0, 7, 8, 15\}$.

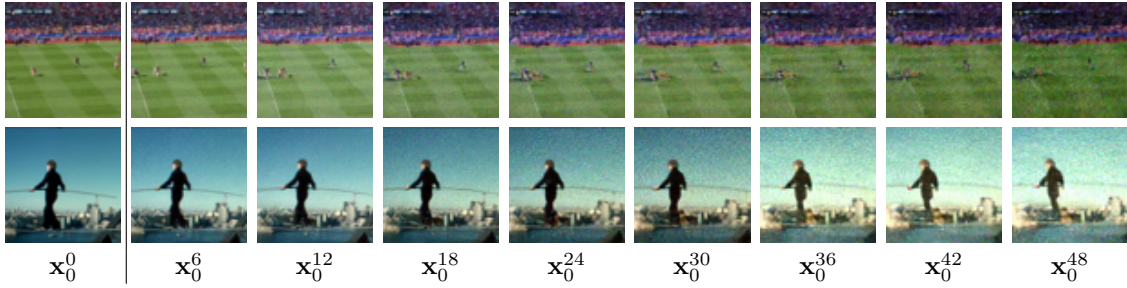


Figure 9: Autoregressive prediction of 50 frames on Kinetics-600.

UCF-101. We compare RaMViD (mixed) with standard RaMViD trained with $K = 4$ (selecting $k \in \{1, \dots, K\}$). We train these two models with the hybrid objective from Nichol and Dhariwal (2021), i.e., using the variational lower bound, and a cosine noise schedule. The results, shown in Table 5, indicate that RaMViD (mixed) performs worse than standard RaMViD. We leave to future work the investigation of the effect of the masking schedule.

Table 5: Performance of RaMViD with $K = 4$ and RaMViD (mixed) with $K = 2$ on prediction ($\mathcal{C} = \{0, 1, 2, 3, 4\}$) on Kinetics-600.

Method	FVD
RaMViD ($K = 4$)	44.30
RaMViD (mixed) ($K = 2$)	49.35

4.6 Autoregressive sampling

While we train our models only on 16 (Kinetics-600) or 20 (BAIR) frames, it is still possible to sample longer sequences autoregressively. By conditioning on the latest sampled frames, one can sample the next sequence and therefore generate arbitrarily long videos. In Fig. 9, we show examples of this autoregressive sampling with RaMViD models trained on Kinetics-600 (the ones we evaluated on standard-length videos in Section 4.2 and Section 4.3). However, we found that this is rather challenging because, at each autoregressive step, the quality of the generated sequence slightly deteriorates. This amplifies over time, often resulting in poor quality after about 30 frames.

5. Conclusion

We have shown that diffusion models, which have been shown to be remarkably powerful for image generation, can be extended to videos and used for several video completion tasks. The way we introduce conditioning information is novel, simple, and does not require any major modification to the architecture of existing diffusion models, but it is nonetheless surprisingly effective. Although the proposed method targets conditional video generation, we also introduce an alternative masking schedule in an attempt to improve the unconditional generation performance without sacrificing performance on conditional generation tasks.

Since we have observed varying performance in different tasks using different masking schemes, an interesting direction for future research is to investigate which masking schedules are more suitable for each task. It would also be interesting to explore in future work whether our conditioning technique is also effective for completion on other data domains. Finally, the focus of this work has been on the diffusion-based algorithm for videos rather than on optimizing the quality of each frame. It has been shown in concurrent works that including super-resolution modules helps create high-resolution videos. Adding a super-resolution module to RaMViD would be a relevant direction for future work.

Acknowledgements

This project was enabled by using the Berzelius cluster at the Swedish National Supercomputer Center (NSC).

References

- Abstreiter, Korbinian, Stefan Bauer, Bernhard Schölkopf, and Arash Mehrjou (2021). “Diffusion-Based Representation Learning”. In: *arXiv preprint arXiv:2105.14257*.
- Acharya, Dinesh, Zhiwu Huang, Danda Pani Paudel, and Luc Van Gool (2018). *Towards High Resolution Video Generation with Progressive Growing of Sliced Wasserstein GANs*. DOI: [10.48550/ARXIV.1810.02419](https://doi.org/10.48550/ARXIV.1810.02419).
- Babaeizadeh, Mohammad, Chelsea Finn, Dumitru Erhan, Roy H. Campbell, and Sergey Levine (2018). “Stochastic Variational Video Prediction”. In: *International Conference on Learning Representations*.
- Babaeizadeh, Mohammad, Mohammad Taghi Saffar, Suraj Nair, Sergey Levine, Chelsea Finn, and Dumitru Erhan (2021). “FitVid: Overfitting in Pixel-Level Video Prediction”. In: *CoRR* abs/2106.13195.
- Batzolis, Georgios, Jan Stanczuk, Carola-Bibiane Schönlieb, and Christian Etmann (2021). *Conditional Image Generation with Score-Based Diffusion Models*. DOI: [10.48550/ARXIV.2111.13606](https://doi.org/10.48550/ARXIV.2111.13606).
- Cai, Ruojin, Guandao Yang, Hadar Averbuch-Elor, Zekun Hao, Serge Belongie, Noah Snaveley, and Bharath Hariharan (2020). *Learning Gradient Fields for Shape Generation*. arXiv: [2008.06520](https://arxiv.org/abs/2008.06520) [cs.CV].
- Carreira, Joao, Eric Noland, Andras Banki-Horvath, Chloe Hillier, and Andrew Zisserman (2018). *A Short Note about Kinetics-600*. DOI: [10.48550/ARXIV.1808.01340](https://doi.org/10.48550/ARXIV.1808.01340).
- Chen, Nanxin, Yu Zhang, Heiga Zen, Ron J Weiss, Mohammad Norouzi, and William Chan (2021). “WaveGrad: Estimating Gradients for Waveform Generation”. In: *International Conference on Learning Representations*.
- Clark, Aidan, Jeff Donahue, and Karen Simonyan (2019). “Efficient Video Generation on Complex Datasets”. In: *CoRR* abs/1907.06571. URL: <http://arxiv.org/abs/1907.06571>.
- Denton, Emily and Rob Fergus (July 2018). “Stochastic Video Generation with a Learned Prior”. In: *Proceedings of the 35th International Conference on Machine Learning*. Ed. by Jennifer Dy and Andreas Krause. Vol. 80. Proceedings of Machine Learning Research. PMLR, pp. 1174–1183.
- Dhariwal, Prafulla and Alexander Quinn Nichol (2021). “Diffusion Models Beat GANs on Image Synthesis”. In: *Advances in Neural Information Processing Systems*. Ed. by A. Beygelzimer, Y. Dauphin, P. Liang, and J. Wortman Vaughan.
- Dockhorn, Tim, Arash Vahdat, and Karsten Kreis (2021). “Score-Based Generative Modeling with Critically-Damped Langevin Diffusion”. In: *arXiv preprint arXiv:2112.07068*.
- Ebert, Frederik, Chelsea Finn, Alex X. Lee, and Sergey Levine (Nov. 2017). “Self-Supervised Visual Planning with Temporal Skip Connections”. In: *Proceedings of the 1st Annual Conference on Robot Learning*. Ed. by Sergey Levine, Vincent Vanhoucke, and Ken Goldberg. Vol. 78. Proceedings of Machine Learning Research. PMLR, pp. 344–356.
- Finn, Chelsea and Sergey Levine (2017). “Deep visual foresight for planning robot motion”. In: *2017 IEEE International Conference on Robotics and Automation (ICRA)*, pp. 2786–2793. DOI: [10.1109/ICRA.2017.7989324](https://doi.org/10.1109/ICRA.2017.7989324).
- Hafner, Danijar, Timothy Lillicrap, Ian Fischer, Ruben Villegas, David Ha, Honglak Lee, and James Davidson (June 2019). “Learning Latent Dynamics for Planning from Pixels”. In: *Proceedings of the 36th International Conference on Machine Learning*. Ed. by Kamalika Chaudhuri and Ruslan Salakhutdinov. Vol. 97. Proceedings of Machine Learning Research. PMLR, pp. 2555–2565.

- Harvey, William, Saeid Naderiparizi, Vaden Masrani, Christian Weilbach, and Frank Wood (2022). *Flexible Diffusion Modeling of Long Videos*. DOI: [10.48550/ARXIV.2205.11495](https://doi.org/10.48550/ARXIV.2205.11495).
- Ho, Jonathan, Ajay Jain, and Pieter Abbeel (2020). “Denoising Diffusion Probabilistic Models”. In: *Advances in Neural Information Processing Systems*. Ed. by H. Larochelle, M. Ranzato, R. Hadsell, M.F. Balcan, and H. Lin. Vol. 33. Curran Associates, Inc., pp. 6840–6851.
- Ho, Jonathan, Tim Salimans, Alexey Gritsenko, William Chan, Mohammad Norouzi, and David J. Fleet (2022). *Video Diffusion Models*. DOI: [10.48550/ARXIV.2204.03458](https://doi.org/10.48550/ARXIV.2204.03458).
- Hu, Anthony, Fergal Cotter, Nikhil Mohan, Corina Gurau, and Alex Kendall (2020). *Probabilistic Future Prediction for Video Scene Understanding*. DOI: [10.48550/ARXIV.2003.06409](https://doi.org/10.48550/ARXIV.2003.06409).
- Hyvärinen, Aapo and Peter Dayan (2005). “Estimation of non-normalized statistical models by score matching.” In: *Journal of Machine Learning Research* 6.4.
- Jiang, Huaizu, Deqing Sun, Varun Jampani, Ming-Hsuan Yang, Erik Learned-Miller, and Jan Kautz (2018). “Super slo-mo: High quality estimation of multiple intermediate frames for video interpolation”. In: *Proceedings of the IEEE conference on computer vision and pattern recognition*, pp. 9000–9008.
- Kahembwe, Emmanuel and Subramanian Ramamoorthy (2020). “Lower dimensional kernels for video discriminators”. In: *Neural Networks* 132, pp. 506–520. ISSN: 0893-6080. DOI: <https://doi.org/10.1016/j.neunet.2020.09.016>.
- Kong, Yu and Yun Fu (2018). *Human Action Recognition and Prediction: A Survey*. DOI: [10.48550/ARXIV.1806.11230](https://doi.org/10.48550/ARXIV.1806.11230).
- Lee, Alex X., Richard Zhang, Frederik Ebert, Pieter Abbeel, Chelsea Finn, and Sergey Levine (2018). *Stochastic Adversarial Video Prediction*. DOI: [10.48550/ARXIV.1804.01523](https://doi.org/10.48550/ARXIV.1804.01523).
- Li, Maomao, Chun Yuan, Zhihui Lin, Zhuobin Zheng, and Yangyang Cheng (2019). “Stochastic Video Generation with Disentangled Representations”. In: *2019 IEEE International Conference on Multimedia and Expo (ICME)*, pp. 224–229.
- Luc, Pauline, Aidan Clark, Sander Dieleman, Diego de Las Casas, Yotam Doron, Albin Cassirer, and Karen Simonyan (2020). *Transformation-based Adversarial Video Prediction on Large-Scale Data*. DOI: [10.48550/ARXIV.2003.04035](https://doi.org/10.48550/ARXIV.2003.04035).
- Lugmayr, Andreas, Martin Danelljan, Andres Romero, Fisher Yu, Radu Timofte, and Luc Van Gool (2022). *RePaint: Inpainting using Denoising Diffusion Probabilistic Models*. DOI: [10.48550/ARXIV.2201.09865](https://doi.org/10.48550/ARXIV.2201.09865).
- Mittal, Sarthak, Guillaume Lajoie, Stefan Bauer, and Arash Mehrjou (2022). “From Points to Functions: Infinite-dimensional Representations in Diffusion Models”. In: *ICLR Workshop on Deep Generative Models for Highly Structured Data*.
- Moing, Guillaume Le, Jean Ponce, and Cordelia Schmid (2021). “CCVS: Context-aware Controllable Video Synthesis”. In: *Advances in Neural Information Processing Systems*. Ed. by A. Beygelzimer, Y. Dauphin, P. Liang, and J. Wortman Vaughan.
- Nichol, Alexander Quinn and Prafulla Dhariwal (July 2021). “Improved Denoising Diffusion Probabilistic Models”. In: *Proceedings of the 38th International Conference on Machine Learning*. Ed. by Marina Meila and Tong Zhang. Vol. 139. Proceedings of Machine Learning Research. PMLR, pp. 8162–8171.
- Niu, Chenhao, Yang Song, Jiaming Song, Shengjia Zhao, Aditya Grover, and Stefano Ermon (2020). *Permutation Invariant Graph Generation via Score-Based Generative Modeling*. arXiv: [2003.00638](https://arxiv.org/abs/2003.00638) [cs.LG].
- Oprea, Sergiu, Pablo Martinez-Gonzalez, Alberto Garcia-Garcia, John Alejandro Castro-Vargas, Sergio Orts-Escolano, Jose Garcia-Rodriguez, and Antonis Argyros (2020). “A review on deep learning techniques for video prediction”. In: *IEEE Transactions on Pattern Analysis and Machine Intelligence*.
- Rakhimov, Ruslan, Denis Volkhonskiy, Alexey Artemov, Denis Zorin, and Evgeny Burnaev (2020). *Latent Video Transformer*. DOI: [10.48550/ARXIV.2006.10704](https://doi.org/10.48550/ARXIV.2006.10704).

- Saharia, Chitwan, William Chan, Huiwen Chang, Chris A. Lee, Jonathan Ho, Tim Salimans, David J. Fleet, and Mohammad Norouzi (2021a). *Palette: Image-to-Image Diffusion Models*. DOI: [10.48550/ARXIV.2111.05826](https://doi.org/10.48550/ARXIV.2111.05826).
- Saharia, Chitwan, Jonathan Ho, William Chan, Tim Salimans, David J. Fleet, and Mohammad Norouzi (2021b). *Image Super-Resolution via Iterative Refinement*. DOI: [10.48550/ARXIV.2104.07636](https://doi.org/10.48550/ARXIV.2104.07636).
- Sahin, Caner, Guillermo Garcia-Hernando, Juil Sock, and Tae-Kyun Kim (2020). *A Review on Object Pose Recovery: from 3D Bounding Box Detectors to Full 6D Pose Estimators*. DOI: [10.48550/ARXIV.2001.10609](https://doi.org/10.48550/ARXIV.2001.10609).
- Saito, Masaki, Shunta Saito, Masanori Koyama, and Sosuke Kobayashi (May 2020). “Train Sparsely, Generate Densely: Memory-Efficient Unsupervised Training of High-Resolution Temporal GAN”. In: *International Journal of Computer Vision* 128.10-11, pp. 2586–2606. DOI: [10.1007/s11263-020-01333-y](https://doi.org/10.1007/s11263-020-01333-y).
- Salimans, Tim, Ian Goodfellow, Wojciech Zaremba, Vicki Cheung, Alec Radford, Xi Chen, and Xi Chen (2016). “Improved Techniques for Training GANs”. In: *Advances in Neural Information Processing Systems*. Ed. by D. Lee, M. Sugiyama, U. Luxburg, I. Guyon, and R. Garnett. Vol. 29. Curran Associates, Inc.
- Saremi, Saeed, Arash Mehrjou, Bernhard Schölkopf, and Aapo Hyvärinen (2018). “Deep energy estimator networks”. In: *arXiv preprint arXiv:1805.08306*.
- Saxena, Vaibhav, Jimmy Ba, and Danijar Hafner (2021). “Clockwork Variational Autoencoders”. In: *Advances in Neural Information Processing Systems*. Ed. by A. Beygelzimer, Y. Dauphin, P. Liang, and J. Wortman Vaughan.
- Sohl-Dickstein, Jascha, Eric Weiss, Niru Maheswaranathan, and Surya Ganguli (July 2015). “Deep Unsupervised Learning using Nonequilibrium Thermodynamics”. In: *Proceedings of the 32nd International Conference on Machine Learning*. Ed. by Francis Bach and David Blei. Vol. 37. Proceedings of Machine Learning Research. Lille, France: PMLR, pp. 2256–2265.
- Song, Yang, Jascha Sohl-Dickstein, Diederik P. Kingma, Abhishek Kumar, Stefano Ermon, and Ben Poole (2021). *Score-Based Generative Modeling through Stochastic Differential Equations*. arXiv: [2011.13456](https://arxiv.org/abs/2011.13456) [cs.LG].
- Soomro, Khuram, Amir Roshan Zamir, and Mubarak Shah (2012). *UCF101: A Dataset of 101 Human Actions Classes From Videos in The Wild*. DOI: [10.48550/ARXIV.1212.0402](https://doi.org/10.48550/ARXIV.1212.0402).
- Sun, Jiangxin, Jiafeng Xie, Jian-Fang Hu, Zihang Lin, Jianhuang Lai, Wenjun Zeng, and Wei-shi Zheng (2019). “Predicting Future Instance Segmentation with Contextual Pyramid ConvLSTMs”. In: *Proceedings of the 27th ACM International Conference on Multimedia*. MM ’19. Nice, France: Association for Computing Machinery, pp. 2043–2051. ISBN: 9781450368896. DOI: [10.1145/3343031.3350949](https://doi.org/10.1145/3343031.3350949).
- Tashiro, Yusuke, Jiaming Song, Yang Song, and Stefano Ermon (2021). “CSDI: Conditional Score-based Diffusion Models for Probabilistic Time Series Imputation”. In: *Advances in Neural Information Processing Systems*. Ed. by A. Beygelzimer, Y. Dauphin, P. Liang, and J. Wortman Vaughan.
- Terwilliger, Adam, Garrick Brazil, and Xiaoming Liu (2019). “Recurrent Flow-Guided Semantic Forecasting”. In: *2019 IEEE Winter Conference on Applications of Computer Vision (WACV)*, pp. 1703–1712. DOI: [10.1109/WACV.2019.00186](https://doi.org/10.1109/WACV.2019.00186).
- Tulyakov, Sergey, Ming-Yu Liu, Xiaodong Yang, and Jan Kautz (June 2018). “MoCoGAN: Decomposing Motion and Content for Video Generation”. In: *Proceedings of the IEEE Conference on Computer Vision and Pattern Recognition (CVPR)*.
- Unterthiner, Thomas, Sjoerd van Steenkiste, Karol Kurach, Raphaël Marinier, Marcin Michalski, and Sylvain Gelly (2018). “Towards Accurate Generative Models of Video: A New Metric & Challenges”. In: *CoRR* abs/1812.01717.
- Vincent, Pascal (2011). “A Connection Between Score Matching and Denoising Autoencoders”. In: *Neural Computation* 23.7, pp. 1661–1674. DOI: [10.1162/NECO_a_00142](https://doi.org/10.1162/NECO_a_00142).

- Voleti, Vikram, Alexia Jolicoeur-Martineau, and Christopher Pal (2022). *MCVD: Masked Conditional Video Diffusion for Prediction, Generation, and Interpolation*. DOI: [10.48550/ARXIV.2205.09853](https://doi.org/10.48550/ARXIV.2205.09853).
- Vondrick, Carl, Hamed Pirsiavash, and Antonio Torralba (2016). “Generating Videos with Scene Dynamics”. In: *Advances in Neural Information Processing Systems*. Ed. by D. Lee, M. Sugiyama, U. Luxburg, I. Guyon, and R. Garnett. Vol. 29. Curran Associates, Inc.
- Vondrick, Carl and Antonio Torralba (2017). “Generating the Future with Adversarial Transformers”. In: *2017 IEEE Conference on Computer Vision and Pattern Recognition (CVPR)*, pp. 2992–3000. DOI: [10.1109/CVPR.2017.319](https://doi.org/10.1109/CVPR.2017.319).
- Walker, Jacob, Abhinav Gupta, and Martial Hebert (2015). “Dense Optical Flow Prediction from a Static Image”. In: *2015 IEEE International Conference on Computer Vision (ICCV)*, pp. 2443–2451. DOI: [10.1109/ICCV.2015.281](https://doi.org/10.1109/ICCV.2015.281).
- Weissenborn, Dirk, Oscar Täckström, and Jakob Uszkoreit (2020). “Scaling Autoregressive Video Models”. In: *International Conference on Learning Representations*.
- Wu, Bohan, Suraj Nair, Roberto Martín-Martín, Li Fei-Fei, and Chelsea Finn (2021a). “Greedy Hierarchical Variational Autoencoders for Large-Scale Video Prediction”. In: *2021 IEEE/CVF Conference on Computer Vision and Pattern Recognition (CVPR)*, pp. 2318–2328. DOI: [10.1109/CVPR46437.2021.00235](https://doi.org/10.1109/CVPR46437.2021.00235).
- Wu, Chenfei, Jian Liang, Lei Ji, Fan Yang, Yuejian Fang, Daxin Jiang, and Nan Duan (2021b). *NÜWA: Visual Synthesis Pre-training for Neural visUal World creAtion*. DOI: [10.48550/ARXIV.2111.12417](https://doi.org/10.48550/ARXIV.2111.12417).
- Xu, Qiangeng, Hanwang Zhang, Weiyue Wang, Peter N. Belhumeur, and Ulrich Neumann (2018). *Stochastic Dynamics for Video Infilling*. DOI: [10.48550/ARXIV.1809.00263](https://doi.org/10.48550/ARXIV.1809.00263).
- Yan, Wilson, Yunzhi Zhang, Pieter Abbeel, and Aravind Srinivas (2021). *VideoGPT: Video Generation using VQ-VAE and Transformers*. DOI: [10.48550/ARXIV.2104.10157](https://doi.org/10.48550/ARXIV.2104.10157).
- Yang, Ruihan, Prakhara Srivastava, and Stephan Mandt (2022). *Diffusion Probabilistic Modeling for Video Generation*. DOI: [10.48550/ARXIV.2203.09481](https://doi.org/10.48550/ARXIV.2203.09481).
- Zeng, Kuo-Hao, William B. Shen, De-An Huang, Min Sun, and Juan Carlos Niebles (2017). “Visual Forecasting by Imitating Dynamics in Natural Sequences”. In: *2017 IEEE International Conference on Computer Vision (ICCV)*, pp. 3018–3027. DOI: [10.1109/ICCV.2017.326](https://doi.org/10.1109/ICCV.2017.326).

Appendix A. Implementation details

A.1 Further details on the method

Fig. 10 presents a detailed sketch of our method. Thanks to the way we introduce conditioning frames, the architecture does not need to be changed compared to unconditional models.

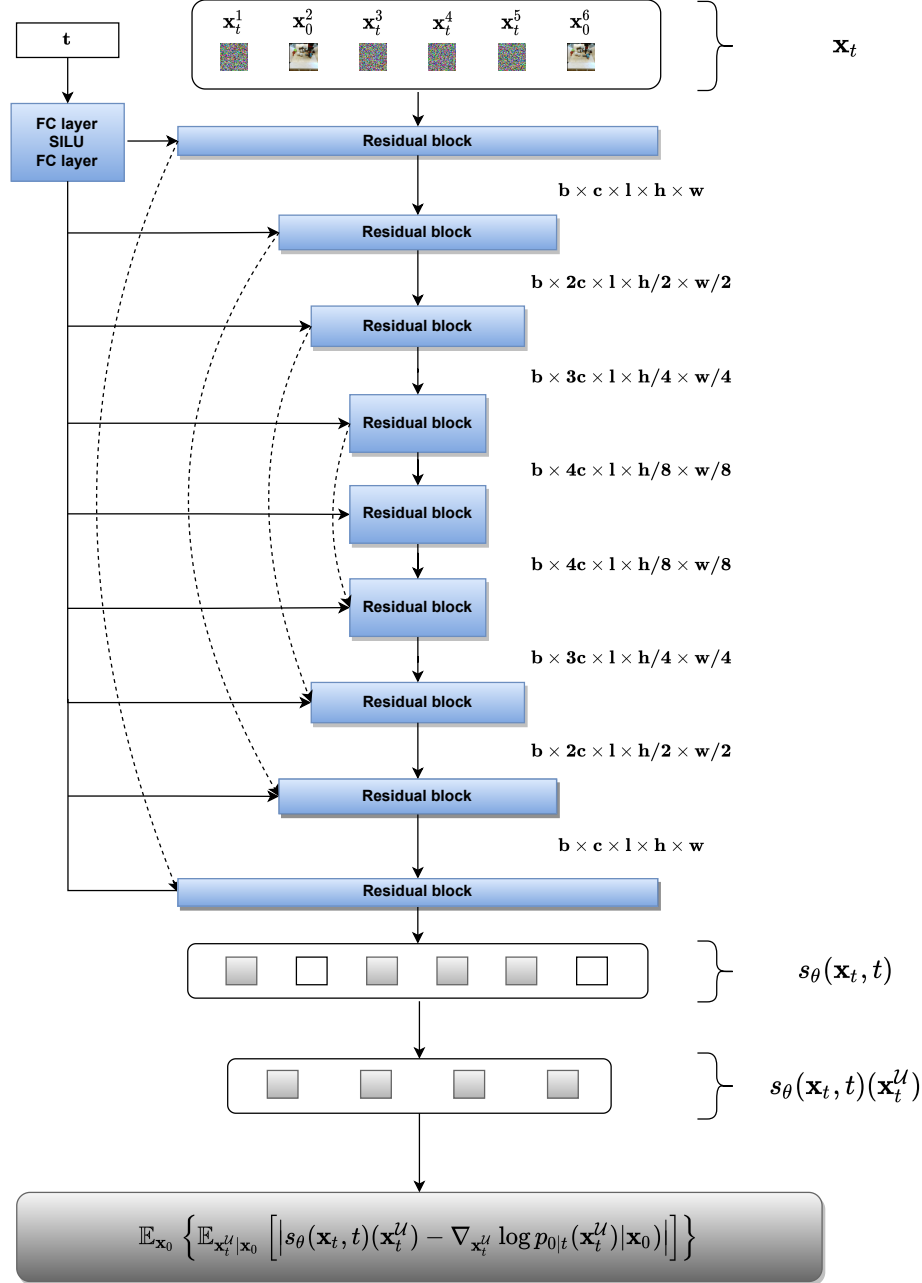


Figure 10: Sketch of our method. In the last step we only compute the loss with respect to the frames that were corrupted with noise. The number of channels c is 128, and l is the video length.

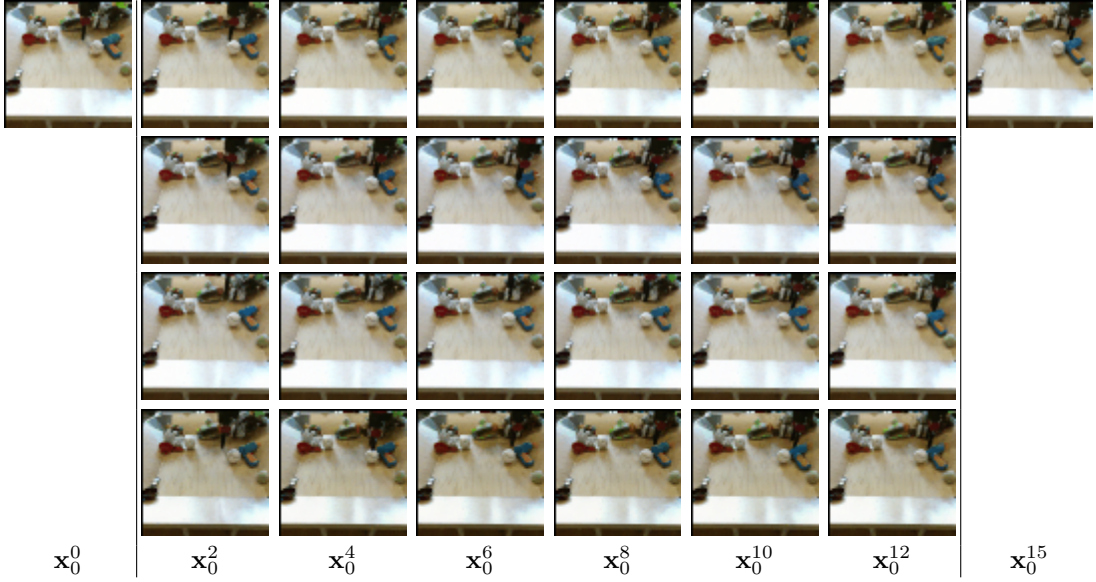


Figure 11: Three different fillings on BAIR given $\mathcal{C} = \{0, 15\}$.

A.2 Configuration

Diffusion. As mentioned, we use the linear noise schedule and the score-based ("simple") objective for all experiments. Only the models presented in Table 5 are trained with a cosine schedule and the hybrid objective from Nichol and Dhariwal (2021), i.e., using also the variational lower bound to guide the diffusion process. All models are trained with 1000 diffusion steps, for sampling we used 750 steps on BAIR, and 500 on Kinetics-600 and UCF-101. Again, the models presented in Table 5 make an exception, as samples are produced with only 250 steps. This is due to the fact that models trained with the hybrid objective need fewer sampling steps and we found that more steps do not improve the results in this case.

Model. As mentioned in Section 4, we use the code base from Nichol and Dhariwal (2021) (MIT license) and their proposed architecture, except that we use $3 \times 3 \times 3$ convolution kernels. In the encoder, we downsample only the spatial dimensions down to 8×8 in three steps. We use 128 channels for the first block and increase it by 128 for each downsampling step. As mentioned in Section 4, we use multi-head self-attention at the resolutions 16 and 8, each with 4 attention heads. For sampling, we found it to be more beneficial to sample from the exponential moving average (EMA) of the weights (Nichol and Dhariwal, 2021). We set the EMA rate to 0.9999.

Appendix B. Additional results

B.1 Results on BAIR

The main evaluation task on BAIR is to predict 15 frames from 1 conditioning frame. But similar to the model trained on Kinetics-600, this model is also able to perform infilling (Fig. 11).

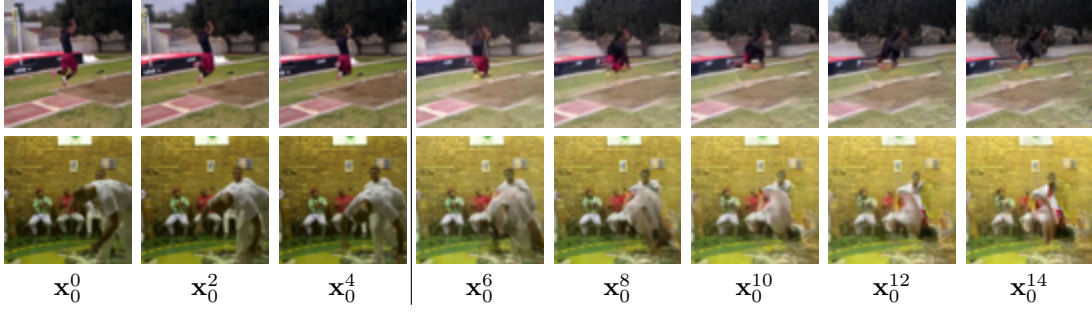


Figure 12: Prediction of 11 frames given the first 5 frames on Kinetics-600 when conditioning on fast moving objects. We can see that the background does get preserved well, while the object itself gets unrealistically deformed.

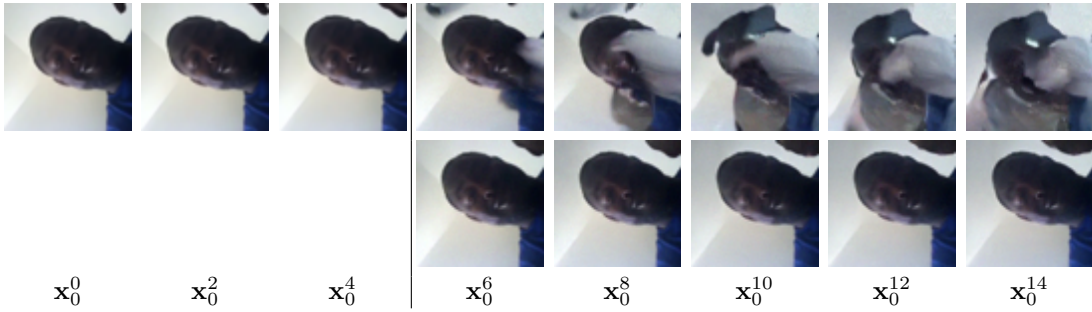


Figure 13: Prediction of 11 frames given the first 5 frames on Kinetics-600. Both predictions are made with the same model and the same number of sampling steps, only the seed is different. We can see that both predictions differ extremely in quality.

B.2 Results on Kinetics-600

Kinetics-600 in practice appears to be the most difficult dataset among those considered here. While our results are state-of-the-art (see Table 2), we do observe failure cases. One of the most common failure cases is fast movement. In that case we often see a deformation of the moving object (see Fig. 12).

A perhaps less easily explainable failure case is the distortion of the entire video. We found that sometimes, depending on the sampling steps and on the seed for initial noise, the same video can have extremely different quality (see Fig. 13).

B.3 Results on UCF-101

Video prediction and infilling also work on the UCF-101 dataset with RaMViD (mixed) and it seems that the model does have similar limitations to the model trained on Kinetics-600. Quantitative results on infilling and prediction can be seen in Table 6. The reason why we have such a high FVD is threefold. First, the FVD decreases when using more test samples, as the estimate of the statistics becomes more accurate. However, we only have 202 test samples, which hurts the FVD score. Second, the model is trained on very few data points, which makes generalizing to unseen data more challenging. Lastly, this model is trained in mixed mode, which we found to decrease performance on video completion (see Section 4.5). However, interestingly, we observe that the

Table 6: Performance of RaMViD (mixed) on UCF-101, when conditioned on different frames during sampling.

Conditioning frames \mathcal{C}	FVD (\downarrow)
$\{0, 1, 2, 3, 4\}$	260.5
$\{0, 1, 14, 15\}$	162.5

performance on infilling is significantly better than on prediction, whereas on Kinetics-600 we see a similar performance on these tasks.

Appendix C. Compute

Each model is trained on NVIDIA A100 GPUs with 40 GB of memory. The models on BAIR are trained with 4 GPUs, a batch size of 32 and a micro-batch size of 8 for 225k iterations (~ 5 days). All other models on Kinetics-600 and UCF-101 are trained on 8 GPUs with a batch size of 64 and micro-batch size of 16. We trained the model presented in Tables 2 and 3 for 500k iterations (~ 9 days), RaMViD (mixed) on UCF-101 for 425k steps (~ 8 days), and the Kinetics-600 models presented in Table 5 for 375k iterations (~ 7 days).

Appendix D. Datasets

The videos in all datasets have more frames than we train on. Therefore we choose random subsequences of the desired length during training.

BAIR robot pushing. The BAIR robot pushing dataset can be used under an MIT license. We use the low resolution dataset (64×64). Since the data is already in the correct size, no preprocessing is necessary. For evaluation we predict one sequence for each of the 256 test videos and compare the FVD to the ground truth. To get a proper evaluation score, we do this 100 times and the final FVD score is the average over all 100 runs. We train on a sequence length of 20.

Kinetics-600. The Kinetics-600 dataset has a Creative Commons Attribution 4.0 International License. The videos have different resolutions, which is why we reshape and center crop them to a 64×64 resolution. For evaluation we take 50,000 videos from the test set and predict a sequence for each of the videos. We then compute the statistics for the ground truth and the predicted videos to obtain the FVD score. We train on a sequence length of 16.

UCF-101. We could not find a license for the UCF-101 dataset. The original frames have a resolution of 160×120 , therefore we resize and center crop the videos to a 64×64 resolution. We only use 13,118 videos in order to have a test set for evaluating the prediction and infilling performance. The test set is created by choosing two random videos for each class. We train on a sequence length of 16 frames. To evaluate prediction and infilling we use a similar method as for BAIR. For each test video, we create 100 samples and report the average FVD. To evaluate the generative performance, we sample 10000 videos unconditionally and compute the Inception Score (IS).⁷ This is repeated three times.

⁷<https://github.com/pfnet-research/tgan2>

Appendix E. Concurrent work

As mentioned in Section 2, three concurrent works on diffusion models for videos were recently made public. Only [Ho et al. \(2022\)](#) and [Voleti, Jolicœur-Martineau, and Pal \(2022\)](#) consider similar tasks as we do. [Ho et al. \(2022\)](#) appears to outperform RaMViD on unconditional video generation on UCF-101, which is not surprising, as we train with the mixed method and therefore the models are mostly trained for conditional generation. [Voleti, Jolicœur-Martineau, and Pal \(2022\)](#) evaluate their method on BAIR with the same procedure we used, and the results reported in their publication suggest that RaMViD outperforms their proposed method with similar computational resources.